materials proceedings

MDPI

Proceeding Paper

The Dual Paradigm of Mining Waste: "From Ecotoxicological Sources to Potential Polymetallic Resources"—An Example from Iberian Pyrite Belt (Portugal) †

Sofia Barbosa [1,*], António Dias [2], Ana Ferraz [3], Sandra Amaro [1], M. Graça Brito [1], J. António Almeida [1] and Sofia Pessanha [2]

[1] GeoBioTec—GeoBioSciences, GeoTechnologies and GeoEngineering & NOVA FCT, 2829-516 Caparica, Portugal; s.amaro@fct.unl.pt (S.A.); mgb@fct.unl.pt (M.G.B.); ja@fct.unl.pt (J.A.A.)
[2] LIBPhys & NOVA FCT, 2829-516 Caparica, Portugal; aad@fct.unl.pt (A.D.); sofia.pessanha@fct.unl.pt (S.P.)
[3] NOVA FCT, 2829-516 Caparica, Portugal; ac.ferraz@campus.fct.unl.pt
* Correspondence: svtb@fct.unl.pt
† Presented at International Conference on Raw Materials and Circular Economy, Athens, Greece, 5–9 September 2021.

Abstract: The main goal of this study was to identify potential chemical elements present in three types of polymetallic mine waste, stored in the old mine site of São Domingos, located in the Iberian Pyrite Belt, Alentejo, Southern Region of Portugal. This study involves the characterization of potential resources in those mine residues, bearing in mind that its reprocessing can facilitate the environmental remediation and rehabilitation activities which are underway at the site. X-ray Fluorescence (XRF) and micro (μ)-XRF 2D mapping surveys were performed. Univariate and multivariate data analysis reveal that differences in compositions are mainly related with element concentration per type of waste. Image processing and clustering analysis allowed the recognition of distinct elemental spatial distribution patterns. Some of these residues, although classified as archeological-industrial heritage materials may present toxicity to the ecological environment and to human health. This fact enhances, therefore, geoethical doubts regarding its remining and exploitability. In this context, a multi-criteria decision analysis considering two geoethical alternatives was performed.

Keywords: mine waste slag; pyrite ash; micro-XRF; clustering analysis and image processing; remining; environmental remediation; mine heritage; Geoethics; multi-criteria decision analysis

Citation: Barbosa, S.; Dias, A.; Ferraz, A.; Amaro, S.; Brito, M.G.; Almeida, J.A.; Pessanha, S. The Dual Paradigm of Mining Waste: "From Ecotoxicological Sources to Potential Polymetallic Resources"—An Example from Iberian Pyrite Belt (Portugal). *Mater. Proc.* **2021**, *5*, 23. https://doi.org/10.3390/materproc2021005023

Academic Editor: Evangelos Tzamos

Published: 23 November 2021

1. Introduction and Motivation for the Study

Nowadays, mining wastes are considered to be an important potential source of critical raw materials (CRMs), such as metals and rare earths. Despite this potential, several critical issues must be correctly characterized in order to enable the effective processing of mining waste. The characterization must address factors that conditionate waste processing such as mineralogy, texture, granulometry and liberation size.

The old "São Domingos" mine is located in the eastern area of the Portuguese Iberian Pyrite Belt (IPB), at the top of the sequence of the volcano-sedimentary complex in which black shales and acidic, basic and intermediate-basic volcanites predominate. The IPB is a particular geological and mining province that is located along much of the southern Iberian Peninsula, from Portugal to Spain. It is about 250 km long and 30–50 km wide, running northwest to southeast from Alcácer do Sal (Portugal) to Sevilla (Spain). The IPB was formed 350 million years ago in the Devonian Period, which is connected to the active and hydrothermal volcanism that led to the formation of a volcanic-sedimentary complex. Originally, the ore mass was composed of pyrite, sphalerite, chalcopyrite, galena, arsenopyrite and sulfosalts. From this mass, pyrite, copper, sulfur, and roasted pyrite were

extracted as products, with an average content of 1.25% copper, 2–3% zinc and 45–48% sulfur [1–3]. The original lithologies were affected by hydrothermal alterations that are marked by the presence of chlorite, silica, and sericite [4]. The deposit was exploited in at least two historical periods: in the Chalcolithic period (Copper Age) by the Phoenicians and Carthaginians [5], mainly for silver extraction [6], and during the Roman period when the superficial part of the mass, which is distinguished by the existence of gossan, was intensively exploited through shafts and galleries for the extraction of copper, silver, and probably gold [1,2,4].

In the modern age, between 1857 and 1966, the deposit was exploited by the company Mason & Barry [3,4]. The products of the mine were cupriferous pyrite, roasted pyrite, sulfur, and copper. During this mining period the average contents were around 3% copper and 50% sulfur [4,5]. The company also produced copper concentrates until 1972 through the cementation process [4]. During this period, some 25 million tons of ore were extracted in total [7].

The former mining area occupies a territory with a maximum extension of more than 20 linear km from North to South and a surface area of more than 6,000 hectares. More than 20 million tons of materials were mobilized, and around 14.7 million tons of waste were accumulated in heaps of up to 14 m high with different types of materials (pyrite, gossan, slag, ash, iron oxides, waste rock, sludge, and rubble) [3,6,8–10]. In [11], the authors estimated that the total of the extracted and the ore-processed waste is about 11 million m^3, which allows for the categorization of these mining wastes into two categories: (1) industrial wastes from processing operations, including Roman and modern slags, iron oxides, foundry ashes, pyrite-rich waste deposits, leaching tank waste and industrial landfills; and (2) mining waste that had piled up as deposits that include gossan and rocks with disseminated sulfides (volcanic host rocks and shales).

The slag piles represent 8% of the mine waste. In geochemical terms, they are rich in Fe and contain relevant contents of Zn, Pb and Cu, as well as low to trace levels of other metals (e.g., Mn, Sb, Co, As, In, Ag, Bi and Ge). The amounts of zinc and arsenic vary from one another, while the Roman slags show higher average values of zinc and lower values of arsenic, compared with the modern slags that contain the opposite concentrations [11,12]. In [8] the authors concluded that there are still significant amounts of metal remaining in both types of slags, dissolved in glass. The ashes from the roasting process are characterized by high contents of numerous elements such as Pb, As, Sn, Sb, Cd, Mo, Se and Cu. The pyrite-rich samples contain high contents of Pb and As, and the iron oxide samples have high contents of Pb and Sb. The leaching tailings are characterized by high concentrations of As, Pb, Se and Zn, and the industrial landfill material has high concentrations of Pb, As and Se. The gossan waste and host rock typically contain high amounts of Pb and As, and they do not have acid potential due to the absence of pyrite or any other sulfate phase. According to local conditions, the total waste from the São Domingos mine has the potential to leach up to 172,514 t of Fe, 10,564 t of S, 6,644 t of Pb, 2,610 t of Zn, 1,126 t of Mn, 1,032 t of Cu 183 t of Cr, 109 t of As, 34 t of Sb and 0.9 t of Cd [8].

Studies that were conducted by [13] revealed, in these wastes, the presence of the critical raw materials Sb, Be, Co, CaF_2, Ge, Ga, Graphite (C), In, Mg, Nb, PGM, REE, Ta, and W. The most interesting concentrations of the detected chemical elements were Sb and Ge, which were up to 30 times the crustal abundance (1.5 $mg \cdot kg^{-1}$). However, there were other valuable elements present in interesting concentrations, some of which are Re, Zn, Fe and Sn. Anglesite, which is probably related to the galena alteration, jarosite, which indicates the erosion of iron sulfides, hematite, and anhydrite, which is generally associated with sulfides and which can be altered to gypsum, were also detected. Some of the identified mineral phases can act as traps for metals. For example, jarosite can incorporate Pb [14]. In the gossan waste piles and volcanic host rocks, interesting concentrations of Au, locally 1 to 4 $mg \cdot kg^{-1}$ [13], were detected.

In our study, a preliminary characterization was performed in order to identify the potential resources (chemical elements) that were present in the three distinct types of

polymetallic mine waste that occur in this old mine site. A recognition of elemental 2D spatial distribution patterns was conducted. As some of the most relevant CRMs in mine waste occur in fine to very fine particle grain size fractions and at the micrometric scale, the application of μ-XRF 2D mapping surveys was tested for this purpose as an elemental characterization technique. Univariate and multivariate data analyses revealed distinct patterns, concentrations, and differences in the compositions of the studied mining waste. The image processing that considered clustering analysis allowed for the recognition of distinct elements and their spatial distribution patterns. The environmental impacts and potential toxicological effects that are generated directly from these wastes are mainly associated with AMD generation and propagation for several km downstream of the mining area [15,16]. In this context, static leaching laboratory experiments were performed. To understand the metal mobility behavior of theses wastes in better environmental controlled conditions, that is, in the future post-rehabilitation stage, the leaching tests were performed using a water solution that is close to neutral and non-reactive (deionized water).

2. Materials and Methods

2.1. Mining Waste Samples

The composite waste samples were collected in three different locations of the mining area. The choice of these samples was based on the different types of materials and their distinct mining period: the Roman period (roman slag), the 20th century mining period (50/60's slags, "60's"), and greywaste (pyrite ash) (Figure 1).

Figure 1. Roman slag (**top**, **left**) distinguished by their aspect: reddish color, and texture tending to be smooth and rolled. The greyish wastes (**top**, **right**), called greywaste, are the mining ashes derived from the cleaning of condensers during the roasting process of pyrite. 60's (at **bottom**) are modern irregular melted dark reddish-brown slags mainly from 50's and 60's decades of the XX Century.

Non-destructive XRF and μ-XRF tests were used to identify the elements that were present and their concentrations in the different types of samples. Thus, it became necessary to reduce the granulometry dimensions of the samples using two pieces of laboratory equipment, a laboratory jaw crusher and an agate ball mill. The samples were pulverized in the ball mill, and the resulting powder was stored in plastic containers that were properly labeled. Samples were homogenized, disaggregated, and quartered by following the usual and appropriate procedures for the preparation of granular samples. Materials were pressed into compacted pellets for measuring purposes (Figure 2). A total of 25 pellets were prepared: 9 of Roman slag, 8 of 60's slag and 8 of greywaste.

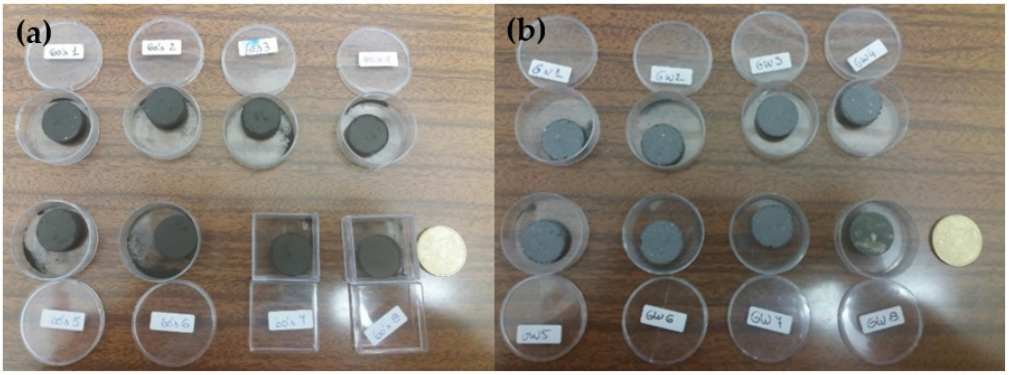

Figure 2. (**a**) Pellet samples of 60's slag, and (**b**) Pellet samples of greywaste.

2.2. XRF and Micro-XRF Analysis

To determine the metal and semi-metal chemical concentrations, a compact hand-held X-ray fluorescence spectrometer Niton (Thermo Scientific Niton XL3p X-ray) was used, which allowed for measurements in parts per million (ppm). Each chemical element has a characteristic emitted energy that is distinct from the other elements, which allows for their identification, evaluation and corresponding quantification [17]. This system had an inbuilt method calibration for the quantification of mining/soil samples.

The technique of μ-XRF was applied by means of an energy dispersive spectrometer M4 TORNADO (Bruker). This benchtop system couples a polycapillary optic to the X-ray source, which allows a spot size of 25 μm (@17.4 keV). The μ-XRF allowed us to obtain the relative concentrations of the elements by comparing spectra and calculating the peak's intensity for each element [18]. The characteristic intensities of the elements in a sample depend on several factors such as the property of the beam, the elements' concentration in the sample, the distribution of the grains, and matrix effects. In the case of the analyzed waste samples, the latter were very difficult to evaluate due to the variability of composition between the samples. Therefore, the results can only be regarded as semi-quantitative. In this case study, the pellet samples were placed in groups inside the spectrometer's chamber. A vacuum pump was used to obtain a 20 millibar atmosphere inside the chamber, preventing radiation absorption in the air in order to enhance the detection limits for lightweight elements [19]. Each sample was analyzed using the multi-point method and the 2D mapping. With the 2D mapping it was possible to obtain a two-dimensional distribution of the identified elements. This distribution analysis can be performed by repeated line scans on equidistant lines by means of the collection of intensities of the previously identified elements, which can be preselected [20]. After obtaining the elements' concentrations with the multi-point analysis and the elements' distribution with the 2D mapping, the data treatment was performed using the inbuilt MQuant software (Bruker). The detection limits and accuracy that were obtained with this system for the IAEA-soil-7 certified reference material are presented in [20].

2.3. Leaching Column-Percolation Tests

Leaching tests can be classified into distinct categories and may be suitable for the prediction of chemical leaching from soil and solid materials such as waste and ore. They can also be utilized to perform initial (small column dimension) hydrometallurgical ore-leaching tests. Compared with other tests like batch-leaching tests, column-percolation tests are time consuming, which is their main disadvantage. On the other hand, column tests resemble field conditions and are suitable to assess the long-term release of chemical constituents from soil and waste into water bodies. Usually, they are used to test the behavior of soil and contaminants under saturated conditions. Column-leaching tests are used to simulate the flow of percolating groundwater through a porous bed of granular material. The flow of the leaching solution may be in either the down-flow or up-flow direction and is either continuous or intermittent. The flow rate is generally accelerated

when compared to natural flow conditions. However, it should be slow enough to allow leaching reactions to occur. Column experiments approximate the flow conditions, particle size distribution and pore structure, leachant flow, and transport of solute found in the field [21–23]. Column methods are more expensive and more operationally complex, but they generate results that reflect real systems that are subject to fluid flow and solute transport. The column test's advantage over other tests, such as batch tests, is that it allows for the observation of high initial concentrations of percolates at low L/S ratios (equilibrium concentrations, that is, concentrations at a certain time after saturation conditions are achieved), and for the possibility of an increased time-dependent release of chemicals, which is required for the prediction of leaching behavior under field conditions.

An adopted procedure of the Standard test method [24] was performed on soil samples using a Behrotest® column elution with a 4-channel hose pump that had a controllable speed (Figure 3). This test method provides for the passage of an aqueous fluid through materials of known mass in a saturated up-flow mode. Close to neutral, non-ionized water was the leachant agent that was used for the test, and granular irregular waste material samples were tested. After the complete saturation of the waste materials inside each column, a rest period of 3 months was applied. The water level inside the columns was controlled to avoid evaporation effects. Measurements of elemental concentrations in the leachate waste materials were performed and compared, respectively, with the concentrations of the original materials.

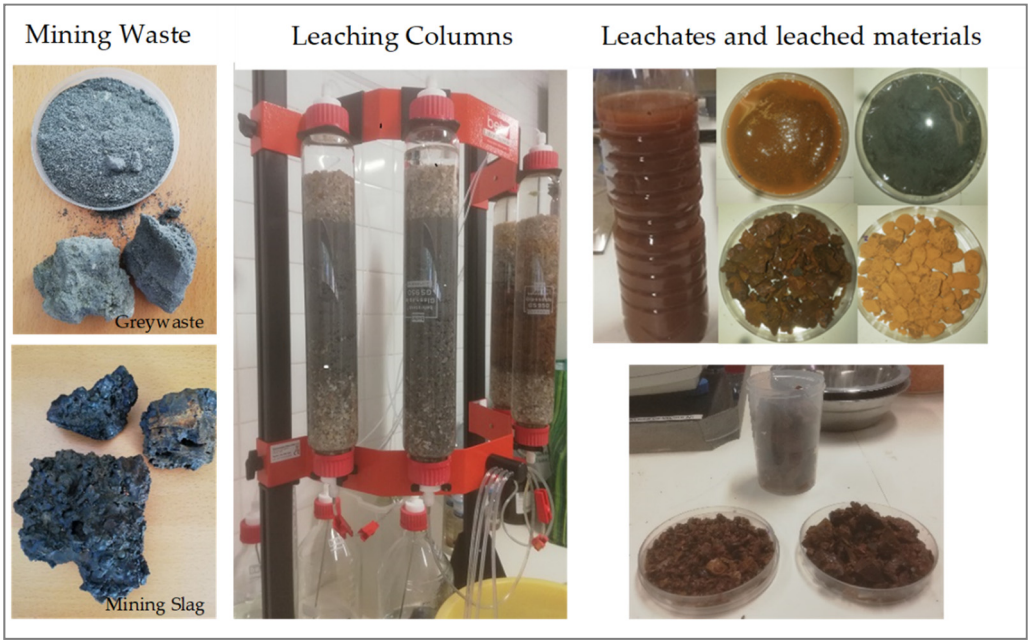

Figure 3. Leaching Column Percolation Tests, original materials, leached and leachates.

2.4. Statistical and Image Analysis

2.4.1. Univariate and Multivariate Analyses

A univariate analysis was developed with regard to the basic statistical parameters of central position, dispersion, and asymmetry. This analysis allowed for the identification of the elements in each type of waste according to distinct grades of concentration. In the multivariate analysis, a Principal Component Analysis was applied to each type of waste, which allowed for the effective identification of distinct groups of elements and their main representative associations. The statistical analyses were performed using R software "R Project for Statistical Computing" [25–28].

2.4.2. Semi-Quantitative RGB Pixel Analysis

The mapping outputs of μ-XRF 2D consisted of 2D image files. The possibilities related to the processing of these image files are, in fact, related to pixel quantification and statistical analysis. In this case study, each image refers to a certain element for which the occurrence and concentration are locally represented by the specific intensity of a certain RGB (Red, Green, Blue) color. The highest elemental concentrations are represented by higher RGB light-color proportions.

The pixel proportion quantifications for each of the distinct RGB colors and their respective intensities, that is, for each of the distinct chemical elements, were established with the R©Countcolors Package [29,30]. This package is the result of a collaboration between Sarah Hooper, Sybill Amelon, and Hannah Weller, and it was originally developed with the aim of quantifying the area of white-nose syndrome infection of bat wings. The R©Countcolors Package allows users to quantify regions of an image by different colors. It is an R package that counts colors within specified color ranges in image files and provides a masked version of the image with the targeted pixels changed to a different selected color by the user. This package integrates techniques from image processing without using any machine learning, adaptive thresholding, or object-based detection, which makes it reliable and easy to use but limited in terms of its application [29,30].

In Countcolors, the principle of the image processing analysis consists of considering each RGB color in three-dimensions, where each color is defined by its coordinates in R (red), G (green) B (blue) axes. The range of each RGB color is thus interpreted in a 3D space. An analysis methodology is defined based on two options: one that considers the upper and lower limits for each color range and draws a box-shaped border around the region of that range (rectilinear range), and another second option that considers the selection of a certain central-color and the search radius around it, and draws a "sphere" to indicate the considered color range (spherical range).

The quantitative RGB pixel analysis that was performed for each 2D image began with the verification of the level of similarity of color intensities according to their respective RGB codes. Each RGB code represents a certain RGB cluster, and thus a certain color intensity. The RGB pixels per cluster were counted using samples of 10,000 pixels from the 2D image. For each RGB code that represented a certain cluster, its frequencies were calculated. In Figure 4, an example of the pixel-counted frequencies for eight distinct color clusters, which represent the existence of an element, is presented. The lighter pixels of the color clusters represent the locations where the element occurs for certain. In this process, the number of clusters and sampling pixels are established by the user.

A methodology based on the application of the R©Countcolors Package's available scripts and its possible interpretations was developed for this specific case study. In this case, the main objective was to estimate the areas that were associated with a certain range of RGB pixels, which represented the locations of certain chemical elements. The lighter color ranges, which were associated with highest color intensities, represented the occurrence of an element. In this methodology, after the selection of the color clusters that were the most representative of a certain element, its frequency of occurrence, as an area inside the image area, can also be estimated. The results are presented in terms of the percentage of the total image area. Due to the possibilities of applying different criteria to identify the elements in the images, it is advisable to reference the percentages between a minimum and maximum of the most probable areas. In fact, the calculated areas can indicate several distinct possibilities that are directly dependent on the number of color clusters and the search criteria, which are user defined. Due to these distinct possibilities, in cases of doubt, it is more correct to suggest the result as a range of probable estimated areas than to present only a unique specific estimated area. The methodology also integrates the possibility of applying search criteria with one-, two-, or three-color clusters simultaneously. When two- and three-color clusters are considered, a search radius is applied to each color. For minimum area calculations, it is advisable either to consider the one-color cluster procedure with spherical or rectilinear search criteria or the two-color

cluster procedure. To calculate the possible maximum estimated areas, it is advisable to simultaneously consider three-color clusters for the estimations (Figure 5). The elemental occurrence is represented by the light-colored clusters in each color image.

Clusters	R	G	B	Frequency (%)
1	0.004	0.537	0.005	15.5
2	0.004	0.298	0.005	6.7
3	0.004	0.403	0.005	15.5
4	0.004	0.481	0.005	16.1
5	0.004	0.356	0.005	10.7
6	0.004	0.214	0.005	2.6
7	0.006	0.510	0.006	15.5
8	0.005	0.446	0.005	17.3

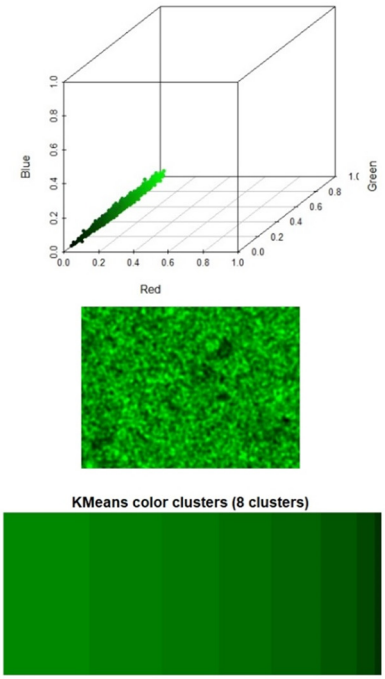

Figure 4. Counting pixels frequencies for the element Si (Silica) considering eight color clusters.

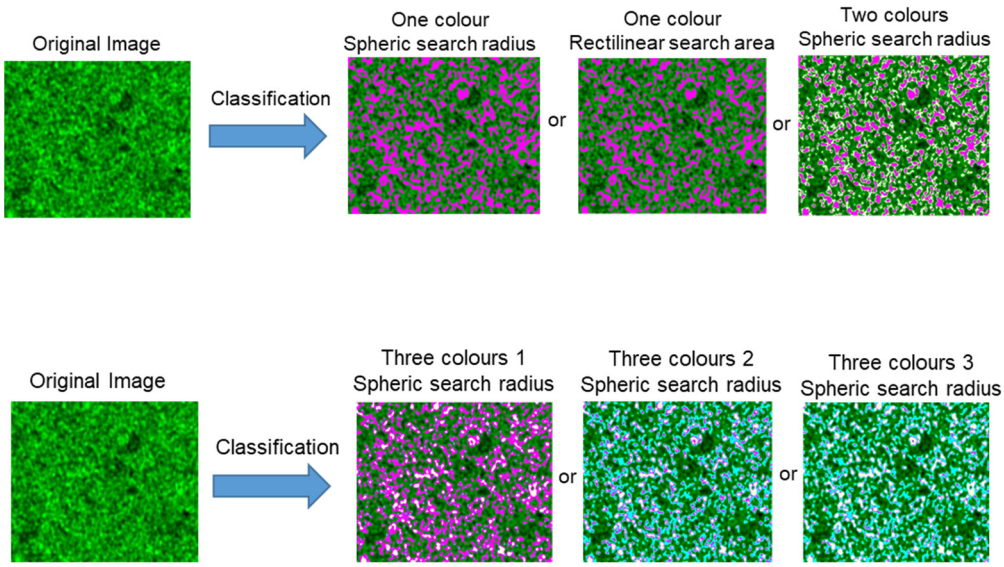

Figure 5. Estimation of the minimum and maximum areas of occurrence of an element.

This methodology allows for an analysis of the images not only qualitatively, but also semi-quantitatively. The uncertainty is mostly associated with the clustering classification and search criteria definitions, which are user-defined.

2.5. Multi-Criteria Decision Analysis (MCDA) Method

The MCDA supports decision-makers in their decisions and is widely used in the fields of management and operational research. There are many MCDA methods, each of them suited for different kinds of decision problems, which can be the prioritization

of projects, the selection of one alternative among many, the selection of several projects with the consideration of precedence between them, or even the rating of alternatives. An MCDA considers the stage at which a problem needs to be structured and modeled, through the definition of alternatives and criteria [31,32]. These criteria are used to evaluate each alternative by means of values, i.e., the data. At that stage, a structured problem, which can be considered a Multi-Criteria Decision Making (MCDM) situation [33], and a suitable method for that kind of problem is applied in order to help with the decision-making process.

In this study, alternatives and criteria were stablished with the aim of reaching a decision regarding the best solution for São Domingos' wastes. These wastes pose a geo-ethical problem, which is: "Should we favor heritage preservation, or should we use mine wastes to extract their elemental and mineral constituents, thereby contributing to an environmental rehabilitation model that is closer to the principles of a circular economy?" To help to solve this problem, the MCDA method that was selected was the Sequential Interactive Method for Urban Systems (SIMUS), which was developed by Munier [31,34].

SIMUS is a hybrid method that combines Linear Programming (LP) with heuristic methods, namely, weighted sum and outranking procedures [33,35]. It is run in two main stages. The first stage (the LP stage) is the application of the Simplex Linear Programming Algorithm that enables the method to find the optimal solutions, if they exist, for each criterion that is used as an objective function of the LP. This process generates a Pareto Efficient Matrix that holds all of the optimal values for the objective functions (criteria used as such), called an Efficient Results Matrix (ERM). Based on these optimal results, the heuristic methods are applied. First, the weighted sum technique is applied to the alternatives, the output of which is the first ranking of the alternatives. Secondly, the method applies the outranking technique for the examination of the dominant alternative from the criteria, i.e., the Project Dominance Matrix (PDM), and the calculation of the difference between the dominant and subordinated alternatives, thereby giving the second ranking of the alternatives.

3. Results and Discussion

3.1. Elemental Identification with X-ray Fluorescence Techniques

The studied mining wastes had similarities regarding the total elements that were present and detected through XRF technique. Fe, K, Ca, Ti, Ba, Cu, Zn, Pb, Sn, As, Sb, and Mn occur in the three types of wastes, despite the different levels of concentrations per waste type. Figure 6 shows the univariate statistics of the main elemental results that were obtained by XRF for the different mining wastes. The very low concentration of iron in greywaste can be explained by the fact that this mining-ash waste is related to the roasting process of pyrite. In addition, tungsten (W) had an interesting behavior, having been present in the Roman slags and the greywaste but not in the 60's slags, which should be reviewed in further studies. The XRF results also revealed the presence of the elements Ga, Ge, Ag, Zr, Rb, Nb, V, Mo, Cs, Te, and Ta in the three types of mining waste materials. However, measurement constraints (equipment and inadequate high-detection limits for these elements) have been a limited the identification of these elements in the studied waste matrices. For such reasons, alternative equipment and chemical identification techniques should be considered in future studies. The technique of μ-XRF allowed us to confirm the elements Al, Si, and S, which were expected to occur in these wastes, Cr in Roman slags, and small amounts of Fe and Bi in greywaste. It should be noted that in [4,8,11] the authors identified distinct minerals in these mining wastes which, at least in part, explain the identified elements. Among others, quartz, pyrite, pyrrhotite, chalcopyrite, galena, distinct iron oxides, glass, gypsum, graphite, pyroxenes, and jarosite were identified.

In Figure 7, the graphical results for the first two dimensions of the Principal Component Analysis (PCA) are presented for Roman and 60's slags, and for greywaste. The results show different associations of elements per type of waste. This fact suggests significant differences in the distributions of chemical elements in the dependence of the waste grains,

according to different mineral compositions and probably varying with granulometry. During Roman times, São Domingos was exploited for the extraction of Cu, Ag and Au. In Roman slags, a higher proportion of Cu and Zn concentrations was found, which was due to the lower efficiency of the processing techniques of the time, while in 60's slags, these elements tended to be present in lower quantities. This is because the processing in modern times was mainly focused on the extraction of Cu- and Zn-based metal concentrates, since the processing techniques were more efficient. In both slag types, sulfur always occurred in high concentrations and had an outlier behavior as a result of the remobilization effects during the mineral processing. In the greywaste, we observed the silica behavior as an outlier, just as with S, and the evidently distinct associations of different metals, mainly Fe-Zn-Cu-Al, which incorporates the structures of the sulfides, and the semi-metals As-Sb-Pb-Sn-Bi, which are usually present in other types of minerals such as sulfosalts, sulfates, and even some other differentiated sulfides (such as Pb or Sn). Greywaste is, in fact, ashes that originated from pyrite roasting or burning in order to produce sulfuric acid. The extraction of sulfur produces, in general, a hematite-rich waste, known as roasted pyrite ash, which contains significant amounts of environmentally sensitive elements in variable concentrations and modes of occurrence [35].

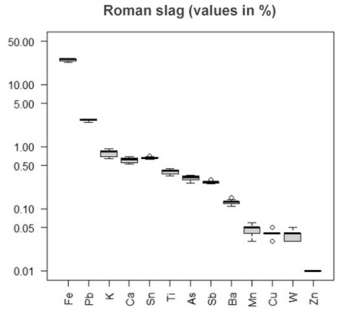

	Element	Average	St.Dev.	Median	Min	Max
Roman	Al	1.39	0.13	1.38	1.19	1.59
	Si	9.17	0.75	9.21	7.74	10.12
	S	38.68	3.61	37.39	34.76	46.16
	K	0.90	0.11	0.90	0.76	1.13
	Ca	0.49	0.10	0.47	0.36	0.66
	Ti	0.54	0.07	0.52	0.46	0.70
	Cr	0.03	0.03	0.02	0.01	0.08
	Mn	0.02	0.01	0.02	0.01	0.03
	Fe	23.55	1.68	23.53	21.22	26.43
	Cu	0.02	0.01	0.02	0.01	0.04
	Zn	0.00	0.00	0.00	0.00	0.00
	As	0.25	0.05	0.23	0.19	0.34
	Sn	0.28	0.02	0.27	0.26	0.33
	Sb	0.12	0.01	0.12	0.10	0.14
	Pb	1.68	0.17	1.73	1.47	1.89

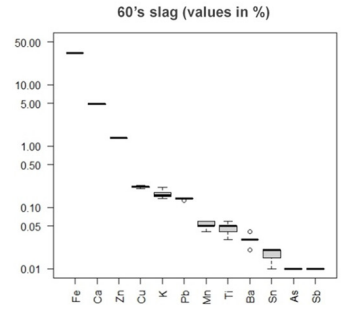

	Element	Average	St.Dev.	Median	Min	Max
60s	Al	0.60	0.07	0.62	0.44	0.64
	Si	6.19	0.67	6.44	4.84	6.80
	S	31.47	6.76	28.38	25.43	46.54
	K	0.14	0.01	0.15	0.12	0.16
	Ca	4.56	0.45	4.61	3.78	5.37
	Ti	0.06	0.01	0.06	0.04	0.07
	Mn	0.03	0.01	0.03	0.02	0.04
	Fe	32.05	3.26	33.20	24.75	35.28
	Cu	0.11	0.02	0.11	0.09	0.13
	Zn	1.12	0.13	1.09	0.93	1.29
	Pb	0.10	0.01	0.10	0.07	0.11

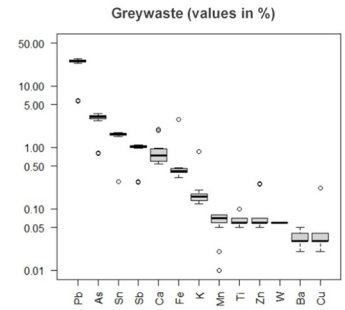

	Element	Average	St.Dev.	Median	Min	Max
Greywaste	Al	0.85	1.31	0.22	0.00	3.77
	Si	4.65	2.69	3.91	1.71	8.70
	S	68.19	5.98	67.97	62.35	80.58
	Ca	0.69	0.99	0.21	0.00	2.70
	Ti	0.11	0.04	0.10	0.06	0.18
	Mn	0.00	0.01	0.00	0.00	0.04
	Fe	1.55	2.78	0.57	0.39	8.43
	Cu	0.04	0.06	0.02	0.01	0.20
	Zn	0.09	0.10	0.06	0.03	0.34
	As	1.31	0.39	1.25	0.81	1.82
	Sn	0.45	0.15	0.47	0.20	0.66
	Sb	0.43	0.11	0.43	0.30	0.58
	Pb	13.20	3.70	13.19	6.02	17.88
	Bi	0.17	0.05	0.16	0.11	0.24

Figure 6. Boxplots and univariate statistics of elemental concentrations measured in Roman slags, 60's slags and greywaste showing variability and dispersion of data per each element.

The statistical results are even more interesting when crossed with the 2D elemental maps that were derived from μ-XRF. Figure 8 shows the processed results of the 2D maps of elemental Cu, Zn, Fe, Al, Si, S, As, Sn, Pb, Sb, and Bi of a greywaste sample without any gridding or milling preparation. Except for Sb, which can be present in specific minerals that are associated with sulfides of Zn, Pb, and Cu, the general tendency of the distinct

elemental associations that were detected in PCA for greywaste is present, particularly in the cases of Fe-Zn-Cu-(Al) and As-Pb-Bi-Sn-(Sb). These preferable associations in 2D patterns are probably explained by mineralogy. Roasting (or burning) temperatures may affect some minerals or remobilize some metals and semi-metals, but may also leave original remaining minerals in the modified waste matrix structure. This may explain, for instance, the spatial behavior of sulfur (S), which is present in a very significant area of the sample and can occur in distinct types of sulfides, sulfosalts and sulfates. Its probable area of occurrence in the image will therefore increase. The roasting (or burning) processing technique may also have restructured the geochemical matrix of the original ore and mobilized some elements, such as Pb and S, which can be more available and have string mobility. This process has certainly contributed to the remobilization and dispersion of S within the waste matrix. It is also important to emphasize that the spatial structure and concentrations of each element significantly varied per type of waste (Figures 6–8). Elements that are associated with alteration and gangue minerals, like Si and Ca, have a very distinct spatial pattern relative to the already discussed metals and semi-metals (Figure 8).

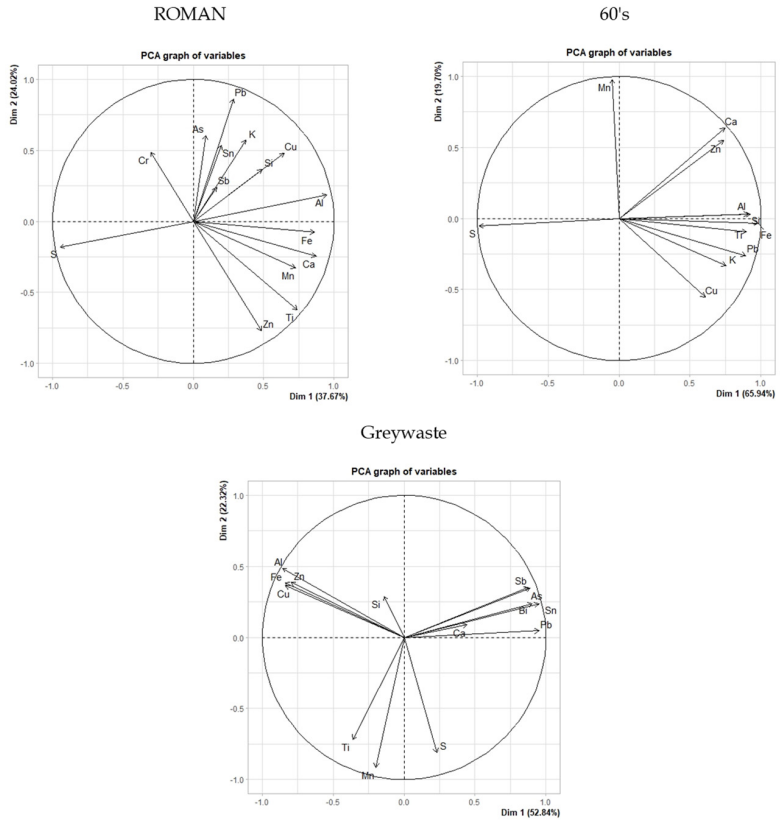

Figure 7. Graphical results of the elements (variables) projection in the first two dimensions of PCA for Roman slags, 60's slags, and greywaste.

In Figure 9, the results of the leaching tests for elements As, Pb and Sb in distinct waste materials are presented. The "LIX" references represent samples of the leached materials after a 3-month-period test. "FL" and "FP" refer to the distinct conditions of Tornado measurement and semi-quantification. It is to say that the results of the performed tests have a double ambiguity regarding their meaning: (1) the potential of element recovery from mining waste with leaching processing techniques, and (2) ecological and human health risk potentialities of the mining waste that was deposited at the site without controlled conditions.

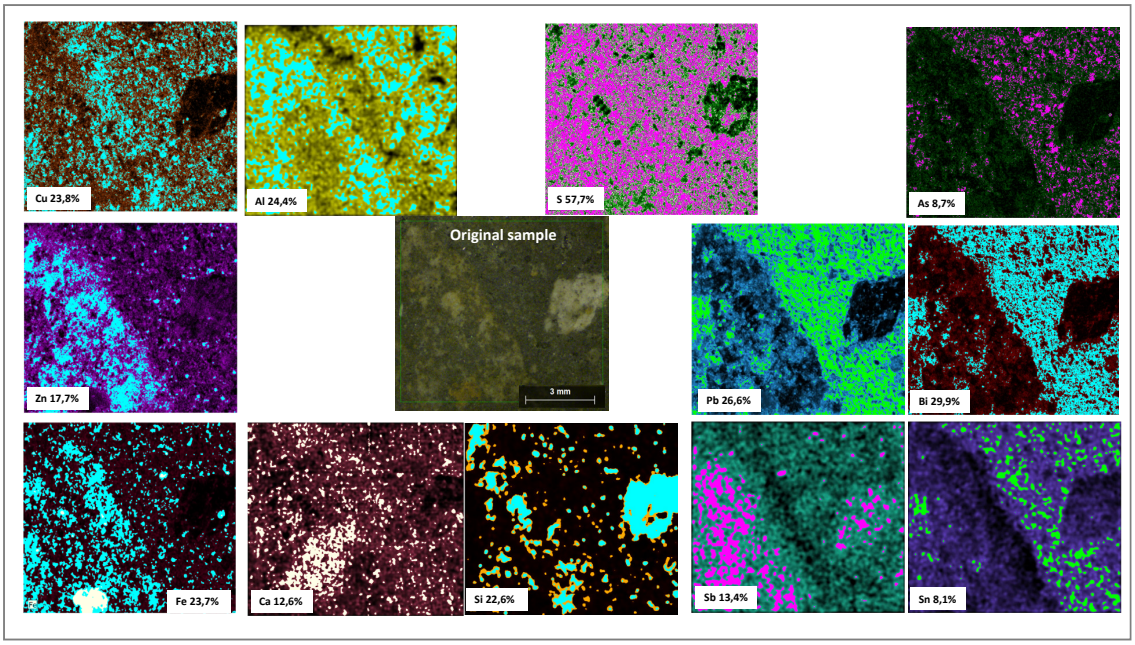

Figure 8. μ-XRF 2D maps of, distinct elemental concentrations in in a greywaste sample without gridding or milling preparation.

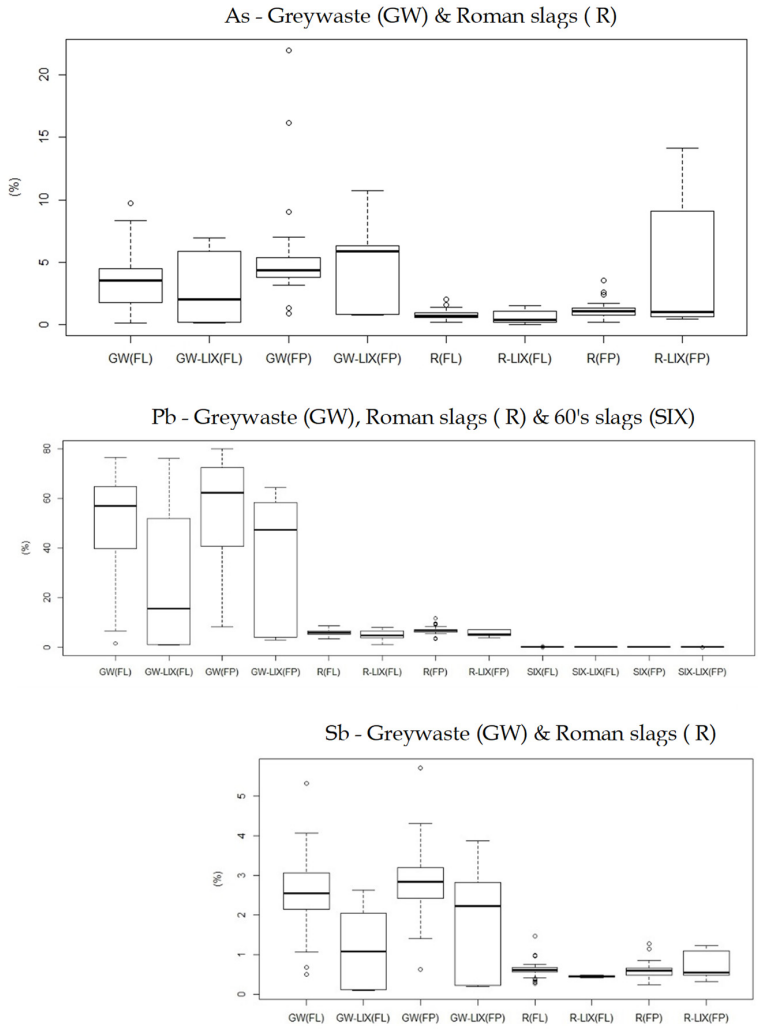

Figure 9. Results of leaching tests for elements As, Pb and Sb in distinct waste materials.

The elements that are presented in Figure 9 are all toxic but are also classified as CRMs in the EU context. The results evidence a much more significant remobilization of As, Pb and Sb from greywaste, compared to the Roman and 60's slags, in conditions that were close to neutral. In fact, these elements presented very low to null mobility leaching effects in the slags. These results evidence that different waste types have distinct behaviors regarding mobility effects. These effects seem to be much more facilitated in the roasted matrix structure of greywaste.

3.2. Results of MCDA

To develop a pre-analysis of the Geo-ethical problem and understand what a good solution for these wastes could be, two alternatives were defined:

1. Environmental rehabilitation without a remining waste project (A1)
2. Environmental rehabilitation with a remining waste project (A2)

To evaluate each of these alternatives, a set of 31 criteria (Table 1) was defined regarding topics such as "Population and environmental benefits and risks," "Land use potentialities and restrictions," "Project costs and economic sustainability," and "Geo-ethical issues, geological and mining heritage." Table 1 corresponds to the Initial Decision Matrix (IDM) where the right columns (A1, A2) regard the values that were attributed by the authors to each criteria, considering their impact on each alternative. From this set of 31 criteria, 7 criteria were not considered (marked with * in Table 1) as objective functions of the LP (Figure 10). Therefore, the references in column "Nr" in Table 1 represent the order of criteria that were introduced in SIMUS (C1, C2, C3, ..., C25, C26, ..., C31). Table 2 shows the meaning of the scale that was used to assess the criteria against the alternatives.

Table 1. Set of criteria used for the MCDA and the data attributed to each criterion to evaluate each alternative.

Topic	Nr	Criteria	A1	A2
Population and environmental benefits and risks	C26 *	Geochemical and hydrogeochemical regeneration and recuperation	3	3
	C1	Ecological regeneration and reclamation	3	5
	C2	Existence and permanence in time of intermediate environmental impacts	−3	−5
	C25 *	Post-rehabilitation environmental impacts	3	3
	C3	Local population benefits regarding improvement of health hazard levels	3	5
	C4	Local population benefits regarding new occupational potentialities	3	5
	C5	Available area for new purposes (left or generated)	3	5
	C6	Risk due to the presence and environmental dispersion of toxic CRM resources on wastes	−3	3
	C7	Dangerous level of new generated waste and by-products	5	−3
	C8	Volume of new generated waste	5	−5
Land use	C9	Land planning policy	−3	3
	C10	Post-mining land use economic potential	3	5
	C11	Potential for private funding	3	5
	C27 *	Potential for public funding	3	3
Project costs and economic sustainability	C12	Project development cost (including I&D)	−3	−5
	C13	Project implementation cost (field work)	−3	−5
	C14	Risk of reprocessing project failure due to technical and costs constraints (penalties in mine waste processing, commodity price variation, market conditions, outflow of goods)	3	−3
	C15	Estimated time for project development (including I&D) and implementation/The time needed to start to enjoy the new PMLU	3	−5
	C16	Economic return derived from project implementation at short to medium term/Contribution to support reclamation costs	−5	5
	C28 *	Economic return derived from project implementation at long term	−3	−3
	C17	Expectations of economic sustainability at short to medium term	−3	3
	C18	Economic sustainability perspective at long term	−5	−3
	C19	Post-rehabilitation environment control costs	−3	3
Geo-ethical issues, geological and mining heritage	C20	Preservation and valorization of mining archaeological heritage	5	−5
	C29 *	Preservation and valorization of geological heritage	3	3
	C21	Promotion and valorization of education and geological knowledge	3	5
	C22	Promotion and safeguarding mine heritage knowledge for present and future generations	5	−5
	C30 *	Protection and valorization of geological characteristics of the site	3	3
	C31 *	Promotion of geoculture and geotourism	3	3
	C23	Promotion of scenic quality highlighting the landscape quality and its diversity	5	−3
	C24	Protection and valorization of natural resources	3	5

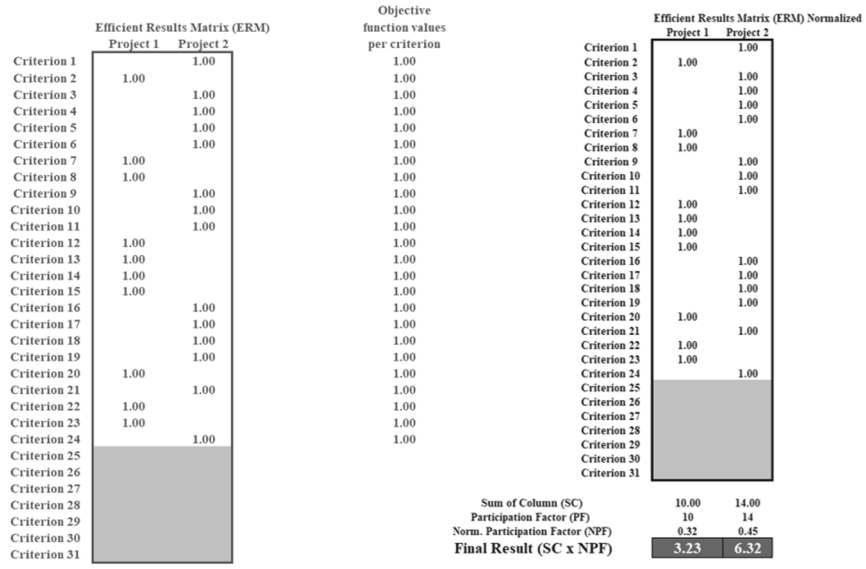

Figure 10. Left: result from the LP stage (ERM), where only 24 criteria were considered as objective functions. Right: first ranking of SIMUS, derived from LP and weighted sum technique applied to columns (alternatives).

Table 2. Scale used to evaluate each criterion on each alternative. Signal significance: +++ Very favorable, ++ Favorable, 0 Indifferent, + Indifferent, – Unfavorable, — Very unfavorable.

Value	Description	Signal
5	Very favorable	+++
3	Favorable	++
0	Indifferent	+-
−3	Unfavorable	–
−5	Very unfavorable	—

The normalized ERM (Figure 10) gives the scores that allow the first rank of alternatives. From the data presented in the last row of Figure 10 (grey cells, white numbers), the most favorable solution is A2 (6.32), which is to consider environmental rehabilitation with a remining waste project.

As previously stated, SIMUS allows for a second result using outranking techniques. Figure 11 presents the results from the outranking stage, where A2 ("Project 2") outranks A1 ("Project 1") by 4 points (brown cell, white numbers). Therefore, the second result provides the same answer as the first result, which is to consider environmental rehabilitation with a remining waste project.

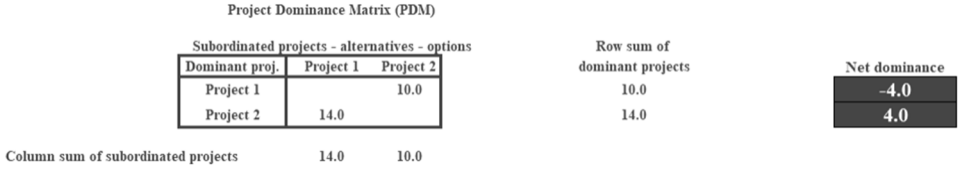

Figure 11. Second result of SIMUS, showing outranking relations.

4. Conclusions, Final Comments, and Remarks

The polymetallic geochemical footprint of the IPB results in the existence of multiple distinct elements in the mining wastes. These wastes are, in fact, "polymetallic wastes." These wastes were studied in order to highlight the occurrence, in distinct mineral and

concentration conditions, of Zn, Cu, Ag, Ag, Pb, Sn, Sb, Se, Al, Mo, Ga, Ge, REE, Sc, In, Ta, Ti, W, Nb, Ba, Be, Bi, Sr, Mg, Cr, Cd, Co, Y and other common mine processing "penalties," such as Fe, Mn, As, Si, and Ca. The long mining history of the site explains the variabilities that were found in distinct wastes. Ore processing, pyrite roasting or burning, cementation, and heap leaching may have contributed to the remobilization of certain elements, to their rearrangement into new molecular constituents, and in some cases, to the destruction of the original mineralogy. The high concentrations of some elements such as Pb, Sn, and As and the detected 2D spatial elemental patterns are indicators of the existence of such modifications. In some cases, it seems that, somehow, the processing actions in the past may have contributed to the concentration of these elements in the waste matrix once they presented patterns with a significant area of distribution. This means that mine waste reprocessing may be relatively more cost-effective compared to what it is expectable.

Environmental impacts and potential toxicological effects that were generated directly from these polymetallic wastes are mainly associated with AMD generation and propagation for several km downstream of the mining area [10,15]. Under these circumstances, static leaching laboratory experiments were performed. The achieved results allowed us to conclude that, despite the polymetallic compositional richness of these mining waste, at least some toxic elements may remain in the material matrix of some of the wastes when conditions are less acidic, or without significant remobilization or dispersion in environmental natural conditions. This can be the case for some mining slags.

Some of these wastes are categorized as archeologic–industrial heritage materials. This fact emphasizes, therefore, the geo-ethical doubts regarding its remining and exploitability. In this context, a multi-criteria decision analysis considering geo-ethical alternatives was performed under two main possibilities: (1) the permanence of these wastes at the old mining site, in more environmental controlled conditions, and without its reprocessing, and (2) the interest in these waste materials being reprocessed. The advantages and disadvantages of these two opposite actions were balanced according to local conditions. From the MCDA results, it is clear that the best compromise solution is to remine the wastes of São Domingos' mine as a component of the environmental reclamation process itself. This action will improve the expectations of economic sustainability in the short to medium term, and of the environmental reclamation process will lead to cleaner solutions for the future area and to lower maintenance costs in the environmental post-rehabilitation stage. For this, however, it is necessary to have more investment at the project stage in order to guarantee the best remining solutions for the wastes, bearing in mind its variability, the distinct depositional conditions at the old mining site and, in some cases, its incomparable compositional differences. However, the expected time to achieve the complete environmental remediation and rehabilitation stage will be longer and some risks of project failure exist. From the characterization studies, not all of the wastes have the same remining potentialities or toxicological risks. Careful decisions about what wastes are to be processed, and under what objectives, must be addressed in the project stage, due to their concentration variability and polymetallic characteristics. The project will have to consider that the action of remining wastes itself will bring local, intermittent, and non-definitive environmental impacts.

In order to better support the decision to remine São Domingos' mine and to help to select a suitable remining method, further detailed and, preferably, semi-quantitative mineralogical and microscopic investigations must be developed in order to have a complete understanding of how each element may occur within the waste matrix relative to the original mineralogical ore composition. Raman microscopy (μRAMAN) is a technique that allows one to obtain composition information that is spatially resolved on the micrometer scale, which is ideal for molecular identification. SEM and QEMSCAN can also be very useful in the context of molecular and mineral characterization, respectively.

Author Contributions: Conceptualization and methodology, S.B., A.D.; writing—original draft preparation, S.B., A.D., A.F., S.A., S.P.; writing—review and editing, S.B., A.D., M.G.B., J.A.A., S.P.; supervision, S.B., A.D. All authors have read and agreed to the published version of the manuscript.

Funding: The research was partially developed for a master thesis, done in the Earth Sciences Department and in Physics Departments of the Faculty of Sciences and Technology (FCT), University NOVA of Lisbon, Portugal. This publication was also supported by FCT—project GeoBioTec/NOVA UIDP/GEO/04035/2020.

Institutional Review Board Statement: Not applicable.

Informed Consent Statement: Not applicable.

Data Availability Statement: This manuscript is a part of a MSc research in Geological Engineering that will be available at https://run.unl.pt before the end of 2021. Remaining data presented in this study can be available on request from the corresponding author and is not publicly available once it is related to ongoing original research.

Acknowledgments: The authors acknowledge the support of LIBPhys, Department of Physics and Department of Earth Sciences of Nova School of Science and Technology for the development of the laboratory work.

Conflicts of Interest: The authors declare no conflict of interest.

References

1. Matos, J.X.; Martins, P.P. Reabilitação ambiental de áreas mineiras do sector português da Faixa Piritosa Ibérica: Estado da arte e perspetivas futuras. *Bol. Geol. Y Min.* **2006**, *117*, 289–304.
2. Carvalho, D.; Goinhas, J.A.C.; Schermerhorn, L.J.G. *Principais Jazigos Minerais do Sul de Portugal, Livro-Guia da Excursão n.º 4. I Congresso Hispano-Luso-Americano de Geologia Económica, Lisboa & Madrid*; Direcç.-geral de Minas e Serviços Geológicos: Lisboa, Portugal, 1971; pp. 59–64.
3. Quental, L.; Bourguignon, A.; Sousa, A.J.; Batista, M.J.; Brito, M.G.; Tavares, T.; Abreu, M.M.; Vairinho, M.; Cottard, F. MINEO Southern Europe environment test site: Contamination impact mapping and modelling: Final Report from MINEO Project—Assessing and monitoring the environmental impact of mining in Europe using Advanced Earth Observation Techniques, September 2002. Available online: http://hdl.handle.net/10400.9/3268 (accessed on 10 January 2020).
4. Matos, J.X.; Pereira, Z.; Oliveira, V.; Oliveira, J.T. The Geological setting of the São Domingos pyrite orebody, Iberian Pyrite Belt. In Proceedings of the VII National Geology Congress, Estremoz, Portugal, 29 June–13 July 2006; pp. 283–286.
5. Oliveira, D.P.S. *A Visitor ' s Guide to the São Domingos Mine/Guia de Visita à Mina de São Domingos*; LNEG: Lisboa, Portugal, 2018.
6. Guita, R.J.N.P. *A Mina de São Domingos (Mértola, Baixo Alentejo, Portugal): Actividade Industrial Moderna 1854–1966*; O Mundo do Trabalho no sul de Portugal: Portimão, Portugal, 2011; pp. 117–132.
7. Oliveira, J.T.; Matos, J.X. O caminho de ferro da Mina de S. Domingos ao Pomarão: Um percurso geo-educacional na Faixa Piritosa Ibérica. Proceedings of the XXIV Encontro de Prof. de Geociências da Assoc. Portuguesa de Geólogos, Beja, Portugal; 2004, p. 19. Available online: https://www.researchgate.net/profile/Jose-Oliveira-30/publication/289127000_Enter_title/links/5689678208ae1e63f1f8f21f/Enter-title.pdf (accessed on 10 January 2020).
8. Mateus, A.; Pinto, A.; Alves, L.C.; Matos, J.X.; Figueiras, J.; Neng, N.R. Roman and modern slag at S. Domingos mine (IPB, Portugal): Compositional features and implications for their long-term stability and potential reuse. *Int. J. Environ. Waste Manag.* **2011**, *8*, 133–159. [CrossRef]
9. Quental, L.; Brito, M.G.; Sousa, A.J.; Abreu, M.M.; Batista, M.J.; Oliveira, V.M.J.; Vairinho, M.; Tavares, T. Utilização de imagens hiperespectrais na avaliação da contaminação mineira em S. Domingos, Faixa Piritosa, Alentejo. In Proceedings of the VI Congresso Nacional de Geologia, Departamento de Ciências da Terra, Monte de Caparica, Portugal, 4–6 June 2003; pp. M33–M36.
10. Quental, L.; Sousa, A.J.; Marsh, S.; Brito, G.; Abreu, M.M. Remote sensing for waste characterisation. In Field Trip Guidebook Multidisciplinary contribution for environmental characterization and improvement at the S. Domingos mining site. In Proceedings of the 9th International Symposium on Environmental Geochemistry, Aveiro, Portugal, 15–21 July 2012; pp. 18–24.
11. Álvarez-Valero, A.M.; Pérez-López, R.; Matos, J.; Capitán, M.A.; Nieto, J.M.; Sáez, R.; Delgado, J.; Caraballo, M. Potential environmental impact at São Domingos mining district (Iberian Pyrite Belt, SW Iberian Peninsula): Evidence from a chemical and mineralogical characterization. *Environ. Geol.* **2008**, *55*, 1797–1809. [CrossRef]
12. Matos, J.X.; Pereira, Z.; Batista, M.J.; Oliveira, D. São Domingos Mining Site—Iberian Pyrite Belt. In Proceedings of the 9th International Symposium on Environmental Geochemistry, Aveiro, Portugal, 15–21 July 2012; pp. 7–12.
13. Batista, M.J.; Matos, J.X.; Figueiredo, M.O.D.; Pereira, T.; Santana, H.; Quental, L. Fingerprints for Mining Products and Wastes of the S. Domingos, Aljustrel and Neves Corvo Mines. In Proceedings of the VIII Congresso Ibérico de Geoquímico/XVII Semana de Geoquímica, Castelo Branco, Portugal, 24–28 September 2011.
14. Figueiredo, O.M.; Silva, T.; Mirão, J.P. Mineroquímica dos sulfatos de ferro secundários: Uma aproximação ambiental em relação com a mina abandonada de S. Domingos. In Proceedings of the VII Congresso Nacional de Geologia, Estremoz, Portugal, 29 June–13 July 2006.

15. Batista, M.J.; Batista, M.G.; Brito, M.M.; Abreu, A.J.; Sousa, L.; Quental, L.; Vairinho, M. Avaliação por modelação em SIG da contaminação mineira por drenagem ácida: S.Domingos, Faixa Piritosa, Alentejo. In Proceedings of the VI Congresso Nacional de Geologia, Departamento de Ciências da Terra, Lisbon, Portugal, 4–6 June 2003; CD-ROM. pp. M6–M10.
16. Quental, L.; Sousa, A.J.; Marsh, S.; Brito, G.; Abreu, M.M. Imaging spectroscopy answers to acid mine drainage detection at S. Domingos, Iberian Pyrite Belt, Portugal. *Comun. Geológicas* **2011**, *98*, 61–71. Available online: http://hdl.handle.net/10400.9/1444 (accessed on 10 January 2020).
17. Beckhoff, B.; Kanngießer, B.; Langhoff, N.; Wedell, R.; Wolff, H. (Eds.) *Handbook of Practical X-ray Fluorescence Analysis*; Springer: Berlin/Heidelberg, Germany, 2006; 863p. [CrossRef]
18. Hall, M. X-ray Fluorescence-Energy Dispersive (ED-XRF) and Wavelength Dispersive (WD-XRF) Spectrometry. In *The Oxford Handbook of Archaeological Ceramic Analysis*; Hunt, A., Ed.; Oxford University Press: Oxford, UK, 2016. [CrossRef]
19. Pessanha, S.; Samouco, A.; Adão, R.; Carvalho, M.L.; Santos, J.P. & Amaro, P. Detection limits evaluation of a portable energy dispersive X-ray fluorescence setup using different filter combinations. *X-ray Spectrom.* **2017**, *46*, 102–106. [CrossRef]
20. Pessanha, S.; Carvalho, M.; Carvalho, M.L.; Dias, A. Quantitative analysis of human remains from18th–19th centuries using X-ray fluorescence techniques: The mysterious high content of mercury in hair. *J. Trace Elem. Med. Biol.* **2016**, *33*, 26–30. [CrossRef] [PubMed]
21. Tiwari, M.K.; Bajpai, S.; Dewangan, U.K.; Tamrakar, R.K. Suitability of leaching test methods for fly ash and slag: A review. *J. Radiat. Res. Appl. Sci.* **2015**, *8*, 523–537. [CrossRef]
22. Meza, S.L.; Kalbe, U.; Berger, W.; Simon, F.-G. Effect of contact time on the release of contaminants from granular waste materials during column leaching experiments. *Waste Manag.* **2010**, *30*, 565–571. [CrossRef]
23. Naka, A.; Yasutaka, T.; Sakanakura, H.; Kalbe, U.; Watanabe, Y.; Inoba, S.; Takeo, M.; Inui, T.; Katsumi, T.; Fujikawa, T.; et al. Column percolation test for contaminated soils: Key factors for standardization. *J. Hazard.* **2016**, *320*, 326–340. [CrossRef] [PubMed]
24. ASTM International Standard. *D4874-95 Standard Test Method for Leaching Solid Material in a Column Apparatus (2014, Withdrawn 2021)*; ASTM International: West Conshohocken, PA, USA, 2014. Available online: http://www.astm.org (accessed on 1 September 2019).
25. Hothorn, T.; Everitt, B.S. A Handbook of Statistical Analyses Using R. CRAN.R-project.org Document. 2005. Available online: https://cran.r-project.org/web/packages/HSAUR3 (accessed on 1 September 2016).
26. R Core Team. *R: A Language and Environment for Statistical Computing*; R Foundation for Statistical Computing: Vienna, Austria, 2013. Available online: http://www.R-project.org/ (accessed on 1 September 2016).
27. Hothorn, T.; Everitt, B.S. *A Handbook of Statistical Analyses Using R*, 3rd ed.; Chapman & Hall/CRC Press, Taylor & Francis Group: Boca Raton, FL, USA; London, UK; New York, NY, USA, 2014.
28. Rahlf, T. *Data Visualisation with R—100 Examples*; Springer: Berlin/Heidelberg, Germany, 2017; ISBN 978-3-319-49751-8.
29. Hooper, E.S.; Weller, H.; Amelon, S.K. Countcolors. An R package for quantification of the fluorescence emitted by Pseudogymnoascus destructans lesions on the wing membranes of hibernating bats. *J. Wildl. Dis.* **2020**, *56*, 759–767. [CrossRef] [PubMed]
30. Weller, H. Package 'Countcolors'. 2019. Available online: https://cran.r-project.org/web/packages/countcolors/countcolors.pdf (accessed on 10 January 2020).
31. Munier, N.; Hontoria, E.; Jiménez-Sáez, F. *Strategic Approach in Multi-Criteria Decision Making*; Springer: Cham, The Netherlands, 2019; Volume 275.
32. Belton, V.; Stewart, T.J. *Multiple Criteria Decision Analysis*; Springer: Boston, MA, USA, 2002.
33. Nigim, K.; Munier, N.; Green, J. Pre-feasibility MCDM tools to aid communities in prioritizing local viable renewable energy sources. Renew. *Energy* **2004**, *29*, 1775–1791. [CrossRef]
34. Munier, N. *Procedimiento Fundamentado En La Programación Lineal Para La Selección De Alternativas En Proyectos De Naturaleza Compleja Y Con Objetivos Múltiples*; Universitat Politècnica de València: Valencia, Spain, 2011; p. 115.
35. Oliveira, M.L.S.; War, C.R.; Izquierdo, M.; Sampaio, C.H.; de Brum, I.A.; Kautzmann, R.M.; Sabedot, S.; Querol, X.; Silva, L.F.O. Chemical composition and minerals in pyrite ash of an abandoned sulphuric acid production plant. *Sci. Total. Environ.* **2012**, *430*, 34–47. [CrossRef] [PubMed]